

# Use of satellite data for land surface assimilation

Matthias Drusch, Klaus Scipal, Erik Andersson, Gianpaolo Balsamo, Thomas Holmes and Patricia de Rosnay

ECMWF, Shinfield Park, Reading  
RG2 9AX, United Kingdom  
M.Drusch@ecmwf.int

## 1 Introduction

Currently, the surface analysis is performed separate from the atmospheric 4D-Var analysis system. The Tiled ECMWF Scheme for Surface Exchanges over Land (TESSEL) is attached to the Integrated Forecast System (IFS) and provides forecasts for snow water equivalent (SWE), skin temperature, soil moisture and temperature (Fig. 1). Analyses are produced for SWE and soil moisture, snow temperature, and top layer soil temperature through a Cressman spatial interpolation and an Optimal Interpolation, respectively. Vegetation parameters and the albedo are obtained from climatologies; other parameters, i.e. sea ice extent and sea surface temperature, are provided by NCEP. Neither the forecast model nor the data assimilation system is currently ready to use satellite observations in the surface analysis effectively.

However, there is a growing demand in accurate estimates of surface variables and a number of applications rely heavily on parameters like SWE and soil moisture, e.g. water resources management, crop modelling, extreme weather forecasting (including floods, droughts and heatwaves) and basic research on the carbon and water cycle. In addition, an accurate surface analysis is valuable for NWP applications including seasonal forecasting (Ferranti and Viterbo (2006)). Due to their spatial and temporal coverage satellite observations will be the key observation source for future surface analysis systems. This paper summarizes (1) current research on the future soil moisture analysis using ASCAT (Advanced SCATterometer) and SMOS (Soil Moisture and Ocean Salinity mission) observations and (2) the recent revision of the SWE analysis.

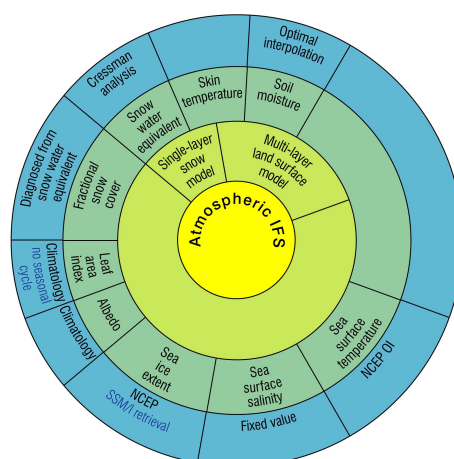


Figure 1: Schematic view on the components of the current surface analysis system used in the medium-range forecast system.

## 2 Soil Moisture

Evapotranspiration is one of the most important parameters for the definition of the thermodynamic and moisture content of the lower troposphere over land. For a given amount of radiative energy available at the surface, the partitioning between the latent heat and sensible heat influences the evolution of the screen level parameters, e.g. 2 m temperature and relative humidity, sub-cloud layer entropy and water, boundary layer clouds, height of cloud base and consequently precipitation. Evapotranspiration is controlled by root zone soil moisture in dry down periods when potential evaporation is high. The soil moisture influence on atmospheric quantities has been shown on the local scale (e.g. [Seuffert et al. \(2002\)](#)), the regional scale (e.g. [Schaer et al. \(1999\)](#)), and the continental to global scale (e.g. [Ferranti and Viterbo \(2006\)](#), [Koster et al. \(2004\)](#), [Shukla and Mintz \(1982\)](#)).

### 2.1 The Effect of Soil Moisture in ECMWF's IFS

In many operational numerical weather prediction applications, the soil moisture analysis is based on the modelled first guess and screen level variables, i.e. 2 m temperature and 2 m relative humidity. In order to quantify the impact of the soil moisture analysis on the quality of the atmospheric forecast, a set of two global 61-day analysis / forecast experiments based on the Integrated Forecast System at the European Centre for Medium-range Weather Forecasts (ECMWF) has been performed for June and July 2002. Analyses and forecasts based on the operational Optimal Interpolation (OI, CTRL experiment) scheme are compared against results obtained from an open loop system (OL), in which soil moisture evolves freely.

Soil moisture analysis increments (i.e. analysis minus modeled first guess) for the root zone have been computed and accumulated for the period from 2 June to 30 July (Fig. 2). In general, the OI analysis scheme adds water to the root zone. Maximum values exceeding 270 mm for the two months period can be found north of the equator in western Africa. Similar values, although on a much smaller spatial scale, are obtained for regions on the Iberian Peninsula. The accumulated analysis increments in the central U.S. and central South America can be as high as 140 mm. There are only very few areas where the analysis removes water from the soil. Minimum values of -95 mm can be found over parts of Argentina. To some extent, the analysis increments are an indicator of the quality of a forecast system: Persistent analysis corrections are a clear sign of systematic model errors. The values shown in Fig. 2 are non-negligible and represent a sizeable part of the terrestrial water budget. It is found that the soil moisture analysis has a significant beneficial impact on the model atmosphere. Temperature forecasts for the Northern Hemisphere up to a level of 700 hPa and up to nine days were significantly improved when the operational analysis was used (Tab. 1).

A comparison of volumetric soil moisture against in-situ observations from the Oklahoma Mesonet reveals, however, that the operational OI system fails to improve both the analysis (Fig. 3) and the subsequent forecast of soil moisture itself. In addition, the system is not able to fully correct soil moisture for errors introduced through wrong precipitation in the background forecasts. Results from the NUDGE simulations are discussed later. Biweekly observations from the Illinois Climate Network support these findings. The results from [Drusch and Viterbo \(2007\)](#) confirm the long assumed (but rarely proven) characteristics of analysis schemes using screen-level variables: The observations are efficient in improving the turbulent surface fluxes and consequently the weather forecast on large geographical domains. The quality of the resulting soil moisture profile is often not sufficient for hydrological or agricultural applications.

### 2.2 Constraining Soil Moisture Using Satellite Observations

Satellite derived surface soil moisture data sets are readily available and have been used successfully in hydrological applications. In order to evaluate the usefulness of remotely sensed soil moisture, which is directly linked to the model's uppermost soil layer and therefore represents a strong constraint in the soil moisture analysis, for NWP applications, a nudging data assimilation experiment with the IFS has been performed for the two months period of June and July 2002. This experimental run incorporates TMI (TRMM Microwave Imager)

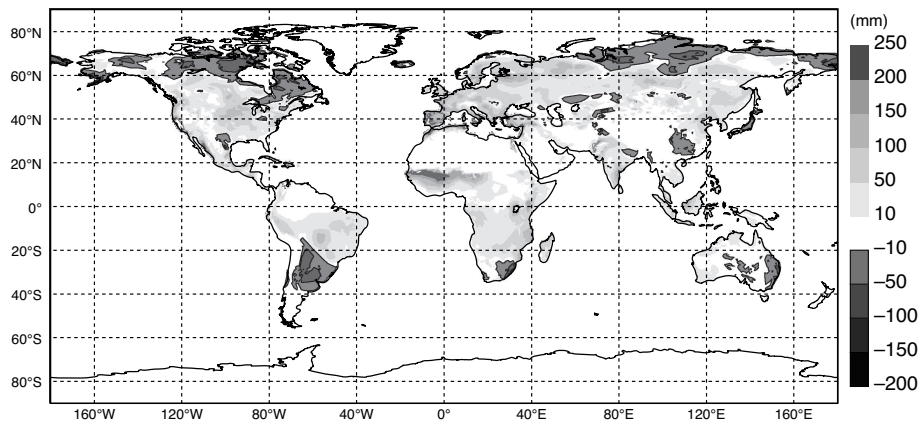


Figure 2: Accumulated root zone (top 1 m soil layer) soil moisture analysis increments (mm) for 2 June to 30 July as computed from the CTRL OI experiment. (from [Drusch and Viterbo \(2007\)](#))

derived soil moisture over the southern United States. The satellite data set has been bias corrected following [Drusch et al. \(2005\)](#); a detailed description of the study can be found in [Drusch \(2007\)](#). Apart from the soil moisture analysis, the system setup reflects the operational forecast configuration including the atmospheric 4D-Var analysis.

Soil moisture analysed in the nudging experiment is the most accurate estimate when compared against in-situ observations from the Oklahoma Mesonet (Fig. 3). As discussed in [Drusch and Viterbo \(2007\)](#), the OI analysis adds water to the surface layer even during periods when the observations indicate lower volumetric soil moisture contents (Fig. 3 a). The nudging experiment using TMI observations improves the surface soil moisture analysis significantly. For the two-months period the correlations between the analyses and the OK Mesonet in-situ observations are 0.44 and 0.81 for the CTRL experiment and the NUDGE run, respectively. The bias is reduced from -0.93 % to -0.15 %. The open loop experiment results in a comparably low bias of -0.14 %. However, this bias is the overall value, which is composed from a dry bias during the first 3 weeks of June and a wet bias during the rest of the period. The TMI data seem to constrain the soil moisture analysis well: During the dry down periods a sufficient amount of water has been added preventing the soil to dry out too quickly. In addition, water can be removed efficiently introducing a considerable amount of variability from one analysis to another, e.g. during the last week of June (Fig. 3 a).

Soil moisture in the second model layer ranging from 7 to 28 cm depth can hardly be compared quantitatively, since the corresponding observation depth is 25 cm. Temporal fluctuations introduced through precipitation are reduced in the observations and there is an offset in the initial conditions of  $\sim 3$  % (Fig. 3 b). Again, the dry down is overpredicted in the different analyses. It is interesting to note that during the second half of June the soil moisture contents from the NUDGE and the CTRL experiments are almost identical. In the CTRL experiment the OI system adds the water directly to layer 2 in the analysis, in the NUDGE experiment the water has been infiltrated from the top layer in the first guess run.

The temporal evolution of root zone soil moisture shows little variability on short time scales; infiltration and the vertical integration tend to filter the signal introduced at the top of the soil column through precipitation. The dominant feature during the study period is a decrease in soil moisture as summer approaches (Fig. 3 c). There is an offset of 1.74 % volumetric soil moisture between the analysed averages and the observations at the beginning of the study period, which can be attributed to deficiencies in the soil hydrology and the selection of the (globally uniform) soil parameters. For the evaluation of the data assimilation experiments this offset has been subtracted from the original observations. The nudging scheme using solely the satellite derived surface soil moisture observations shows the best overall performance with a correlation of 0.94 and a dry bias of 0.4 % when compared against the adjusted observations. The monthly trend is very well represented and even for

Area	Height[hPa]	Forecast time [hours]				
		24	72	120	168	216
N. Hemisphere	1000	0.1 / 0.1 %	0.1 / 0.1 %	0.1 / 0.5 %	2.0 / 10.0 %	- / 1.0 %
	850	0.1 / 0.1 %	0.1 / 0.1 %	0.1 / 5.0 %	- / - %	- / 5.0 %
	700	- / 5.0 %	2.0 / 1.0 %	- / - %	- / - %	- / 10.0 %
Europe	1000	0.1 / 0.1 %	0.1 / 0.1 %	0.2 / 0.1 %	- / - %	- / - %
	850	0.1 / 0.1 %	0.1 / 0.1 %	5.0 / 5.0 %	- / - %	- / - %
	700	- / - %	- / 10.0 %	- / - %	- / - %	- / - %
East Asia	1000	0.1 / 0.1 %	0.1 / 0.1 %	5.0 / 0.1 %	- / 5.0 %	0.5 / 0.5 %
	850	0.1 / 0.1 %	5.0 / 0.1 %	2.0 / 5.0 %	- / - %	0.1 / 0.2 %
	700	2.0 / - %	- / - %	- / - %	- / - %	- / 5.0 %
N. America	1000	0.1 / 0.1 %	1.0 / 0.1 %	- / - %	- / - %	- / - %
	850	0.1 / 0.1 %	0.2 / 0.1 %	- / - %	- / - %	- / - %
	700	- / 5.0 %	- / - %	- / - %	- / - %	- / - %

Table 1: Significance levels for the *t*-test (first value) and sign-test (second value). Temperatures from the CTRL and OL experiment are compared based on rms forecast errors. The numbers represent cases where the CTRL experiment is better than the OL experiment. Dashes indicate cases for which no significant difference has been found.

shorter periods (weeks) the agreement between the temporal change of soil moisture in the observations and the analysis is reasonable.

In Fig. 4 medium-range forecasts up to day 6 for 2m temperatures and relative humidity have been analysed. For the CTRL run, the 24-hour forecast yields a correlation of 0.87 for relative humidity and 0.91 for air temperature. For the 144-hour forecasts the corresponding values are 0.42 and 0.70, respectively. The nudging scheme results in higher correlations for the first 3 days and lower correlations for forecast days 4 to 6 (Fig. 4 a,c). However, the differences between the three experiments are rather small and are not significant at the 95 % confidence level due to the small size of the data sample. The systematic errors increase with forecast time. Overall, the CTRL experiment has the lowest dry bias in relative humidity and the lowest warm bias in temperature. The NUDGE and OL experiments perform systematically worse over the forecast period with the NUDGE experiment showing better results than the OL runs (Fig. 4 b,d). Again, the differences between the forecasts are small with a maximum value of 2.2 % relative humidity between CTRL and OL at day 6. For air temperature a maximum difference of 0.32 K has been obtained. Furthermore, Drusch (2007) shows that the soil moisture analysis influences local weather parameters including the boundary layer height and cloud coverage.

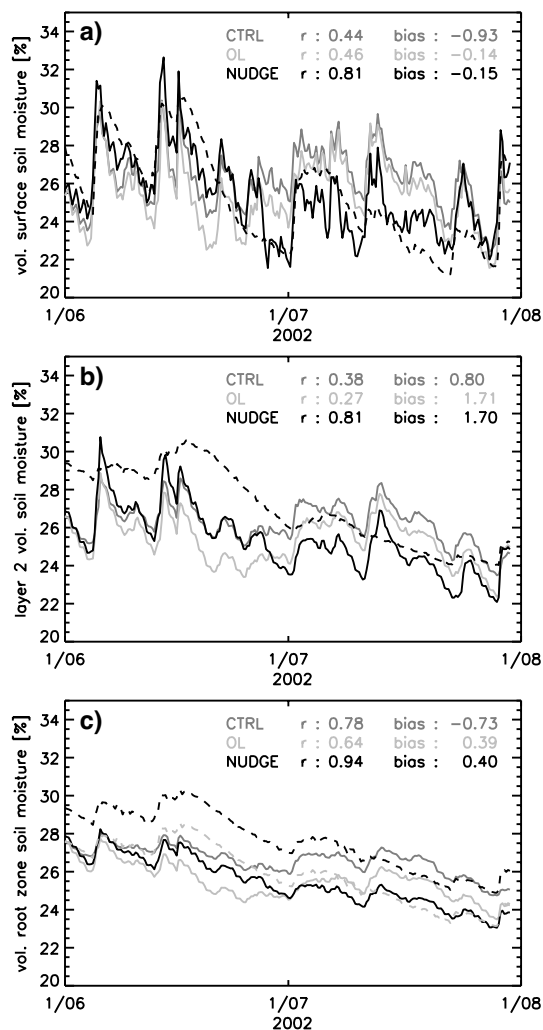


Figure 3: Soil moisture evolution (6-hourly values) during the study period for the surface layer (a), the second layer (b), and the rootzone (c). The lines represent: (1) observations from the OK Mesonet system (dashed black curve), (2) model results from the Open Loop set up (light gray line), (3) analysed values from CTRL OI experiment (dark gray line), and (4) analysed values from the NUDGE run (black line). In c), the dashed grey line represents the observations corrected for the offset in the initial conditions.

### 2.3 A Surface Analysis System for (Future) SMOS Observations

SMOS is the first ever satellite mission designed to provide direct information on surface soil moisture. The observations will therefore constrain the model soil moisture much stronger than the screen level variables. However, the current operational OI analysis system is not very well suited to use multiple observation types at different observation times. Consequently, it is planned to introduce a new land surface data assimilation system, which is fully integrated in the IFS but not part of the atmospheric 4D-Var.

This revised surface data assimilation system will be based on the simplified extended Kalman filter (SEKF). The SEKF has been used by the German Weather Service DWD (Hess (2000)) and within the framework of the European Land Data Assimilation Study (ELDAS, Seuffert et al. (2004)). It is envisaged to run two 12-hour assimilation cycles in parallel to the atmospheric 4D-Var analysis. The future soil moisture analysis will be based on the modelled first guess, 2m temperature and relative humidity analyses, surface soil moisture from ASCAT (see next section), and L-band brightness temperatures from ESA's Soil Moisture and Ocean Salinity (SMOS) mission (Kerr et al. (2001)).

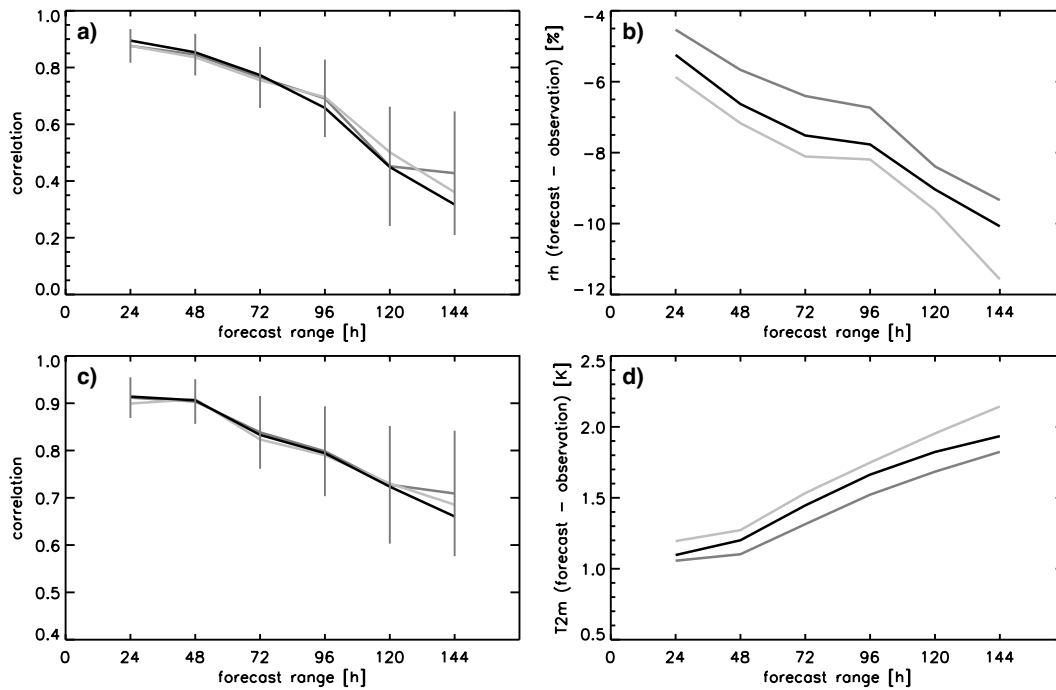


Figure 4: Correlation and bias between forecasts and observations as a function of forecast time. The upper panel presents results for relative humidity, the lower panel air temperature. Forecast basetime is 12 UTC. The CTRL, OL, and NUDGE experiments are represented through dark grey, light grey, and black lines, respectively.

For the assimilation of brightness temperatures a land surface emissivity model is needed as an observation operator transforming the modelled first guess into observation space. At ECMWF, the Community Microwave Emission Model (CMEM) has been developed and calibrated using historic data from the US Skylab Mission in 1973 and the ERA-40 re-analysis (Drusch et al. (2007)). In order to define errors in the model first guess a sensitivity study based on CMEM and standard output from the operational weather prediction system has been performed (Holmes et al. (2007)).

We focus on uncertainties introduced through: (1) the parameterizations of the radiative transfer model, (2) auxiliary geophysical quantities for the radiative transfer computations, and (3) an imperfect NWP model. It is found that the vegetation model and the dielectric model introduce uncertainties, which are on average well below 10 K for most areas of the globe. The biggest error in brightness temperature is likely related to the use of an auxiliary vegetation database which results in differences of -20 to +20 K in our simulations.

In order to quantify the uncertainty in the first guess that is related to an imperfect NWP model we study the variability in  $T_{Btoa}$  that is associated with the uncertainty in the initial state of the Ensemble Prediction System (EPS). EPSs are practical tools designed to assess the predictability of the daily atmospheric flow. More generally, they can be used to predict the time evolution of the probability density function of forecast states. Ensemble systems should be designed to simulate the effect of all sources of forecast errors. In particular, they should simulate the effect of uncertainties in the knowledge of the initial state of the system and the effects of the approximations made in numerical weather prediction models. In order to quantify the uncertainty in the first guess that is related to an imperfect NWP model we study the variability in  $T_{Btoa}$  that is associated with the uncertainty in the initial state of the EPS. The variance in  $T_{Btoa}$  calculated from the 50 members of the EPS (48-hour forecasts from 12 UTC basetime for day 1 and 15 of each month in 2005) will be used as a qualitative indicator of regions where both the uncertainty in initial conditions is high and the sensitivity of a satellite-borne L-band radiometer to soil moisture will be high.



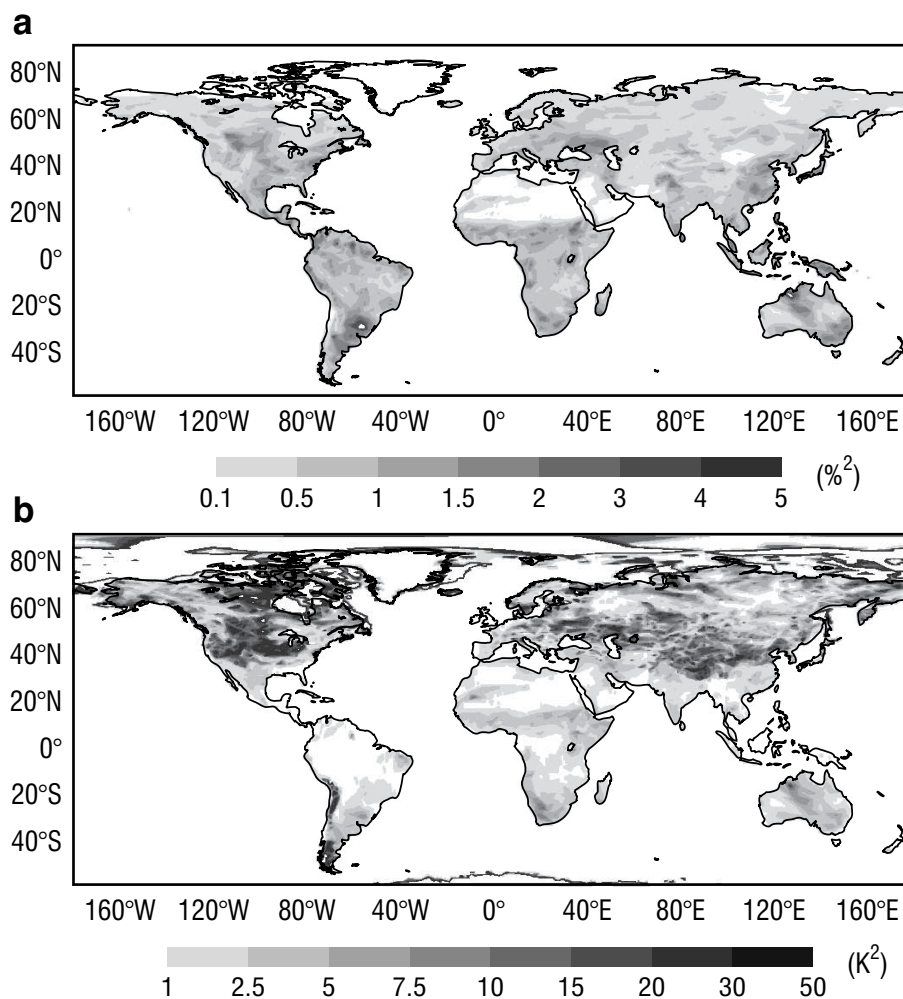


Figure 5: Mean of the variances in volumetric soil moisture content [%<sup>2</sup>] and  $T_{B_{toa,h}}$  [K<sup>2</sup>] of day 1 and 15 for every month of 2005 at 12PM.

The average of the 24 variance maps is shown in Fig. 5 for volumetric soil moisture (a) and horizontally polarized brightness temperature (b). For large parts of the globe the variance in volumetric soil moisture ranges from 0 to 1.5 %<sup>2</sup> with the lowest values in deserts. Areas with higher variance are limited in size and are most likely related to the impact of one-time events. The uncertainty in soil moisture does not translate directly into variability in  $T_{B_{toa,h}}$ : In sparsely vegetated areas where SMOS observations are most sensitive to soil moisture this variance in soil moisture (and other surface state variables) will fully propagate into brightness temperature variances (e.g. over the Central U.S.). Dense vegetation (e.g. rain forest) and the presence of open water bodies will result in a reduced variance in brightness temperature space.

## 2.4 Introducing Scatterometer Derived Soil Moisture

Scatterometer derived soil moisture has been available through the ERS-1/2 missions for almost a decade (Wagner (1998)). From 2008 onwards, a similar data set will be produced in near real time based on ASCAT measurements. It is planned to use the data together with screen level variables and SMOS brightness temperatures in the future Kalman filter surface analysis. However, the most accurate scatterometer derived product is the surface soil moisture index, which has to be transformed to volumetric soil moisture before it can be used in the surface analysis. In order to establish reliable relationships between model soil moisture fields and the

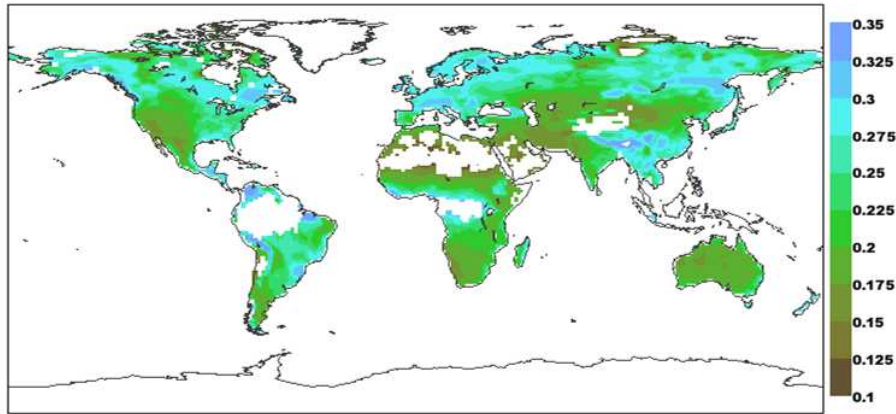


Figure 6: Intercept  $a$  of the linear CDF transformation.

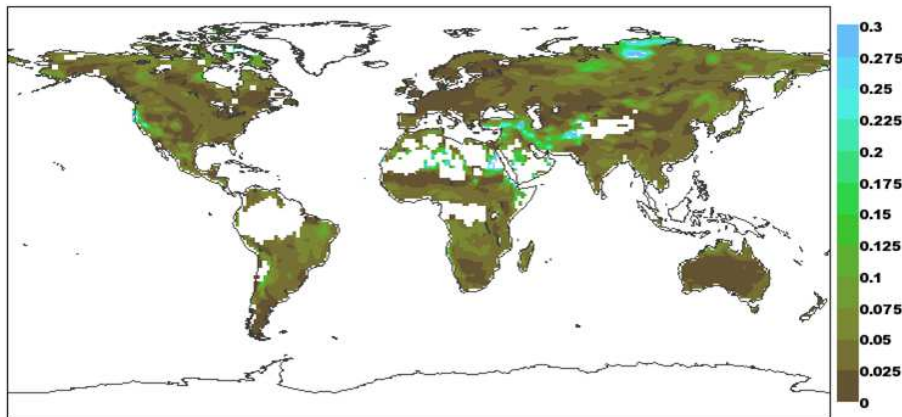


Figure 7: Slope  $b$  of the linear CDF transformation.

scatterometer derived indices, CDF matching as described in [Drusch et al. \(2005\)](#) was applied to 10 years of ERA-40 and ERS-1/2 data. It was found that a linear transformation gives satisfactory results:

$$\begin{aligned}\theta_S &= a + b \times \theta_S \\ a &= \overline{\theta_M} - \overline{\theta_S} \times \frac{\sigma_{\theta_M}^2}{\sigma_{\theta_S}^2} \\ b &= \frac{\sigma_{\theta_M}^2}{\sigma_{\theta_S}^2}\end{aligned}$$

with  $\theta_S$  the transformed satellited derived soil moisture,  $\theta_S$  the satellite based soil water index, and  $\sigma_{\theta_M}^2$  and  $\sigma_{\theta_S}^2$  the variance of the model and satellite data sets, respectively. Intercept  $a$  and slope  $b$  are local coefficients, which were derived for each ERA-40 model grid box. Global maps of intercept  $a$  and slope  $b$  are given in Figs. 6 and 7. It is worth noting that both  $a$  and  $b$  exhibit a spatial structure, which could be related to geophysical parameters; more research is needed to understand these patterns. Figure 8 shows the global distribution of the local (grid box) correlations between the ERA-40 top layer soil moisture and the ERS product for the period from 1992 to 2001. Values between 0.4 and 0.8 have been found in previous validation studies using model fields and observational data sets and have been considered as good. Tropical forests have been masked, since the C-band observations are insensitive to soil moisture changes in these regions. Problems also occur over desert areas, which area characterized by correlations around 0.



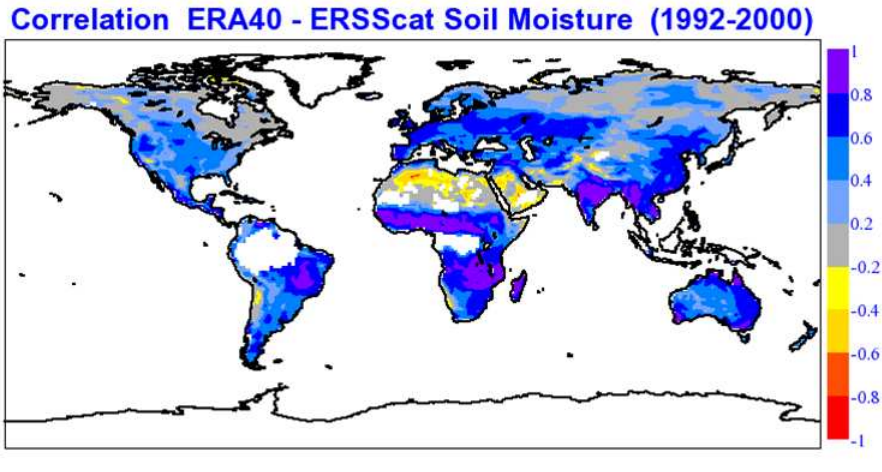


Figure 8: Correlation between ERS scatterometer derived surface soil moisture and ERA-40 top layer soil moisture.

Operational monitoring of the ASCAT derived soil moisture data set will start early 2008.

### 3 Snow

The current ECMWF snow depth analysis is operational since 1987, with modifications in 2001 and 2004. The snow depth analysis  $S^a$  is performed using a Cressman spatial interpolation (e.g. Daley (1991)):

$$S^a = S^b + \frac{\sum_{n=1}^N (S_n^o - S^b)}{\sum_{n=1}^N w_n} \quad (1)$$

where  $S^o$  are the snow depth observations from N SYNOP reports,  $S^b$  is the first guess (i.e. the 6- or 12-hour forecast), and  $S^b$  is the first guess field at the observation point. The weights  $w_n$  are defined through (1) a weighting function depending on the horizontal distance between observation and grid point and (2) a weighting function depending on the vertical displacement (i.e. the model grid point height minus observation height). For a detailed description of the analysis including the quality checks the reader is referred to Drusch et al. (2004).

Snow analyses are performed every 6 hours before the 12-hourly 4D-Var analysis for the atmosphere starts. The 4D-Var 12-hour assimilation window for the atmospheric analysis covers 09 (21) UTC to 21 (09) UTC. As a consequence, the snow analyses are based on the 6-hour and 12-hour forecasts (first guess) from 06 UTC and 18 UTC forecast base times and the observations collected in the 6-hour time period around the analysis time. The first guess for 06 UTC and 18 UTC (i.e. the 12-hourly forecasts) are updated with the analysis increments from the previous analyses at 00 UTC or 12 UTC. A schematic view of the implementation is given in Fig. 9. Prior to 2004, no satellite data have been used and the analyses were relaxed to a climatology. From 2004 onwards, satellite derived NOAA NESDIS snow extent is used in addition to the conventional ground based observations and the model forecast. Areas for which the model first guess is snow free and the NOAA NESDIS product contains snow are updated with a snow depth of 100 mm. Snow free grid boxes in the NOAA NESDIS product enter the analysis as observations with 0 mm snow depth. The relaxation to climatology is omitted since it is expected that the satellite data can replace the role of snow depth climatological data in correcting for the model bias.

Figure 10 shows four resulting snow analyses for March 6, 2004. The 00 UTC analysis (upper left image) is based on a 6-hour forecast from 18 UTC. Over Europe, there are hardly any conventional observations available

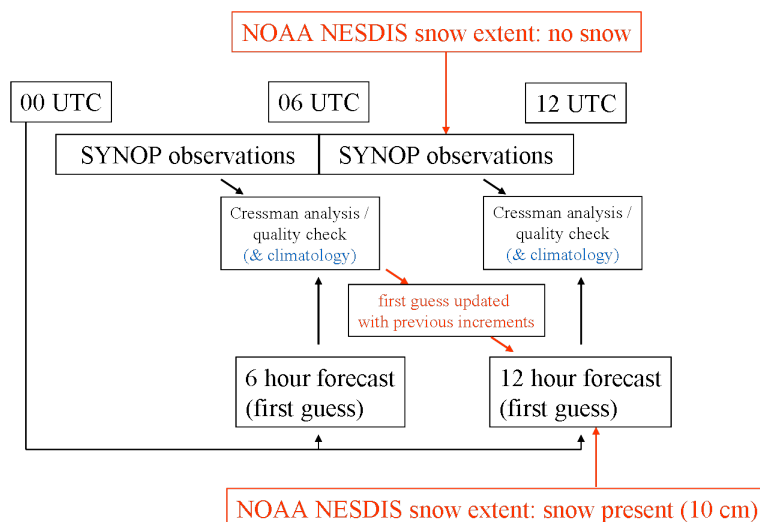


Figure 9: Schematic view of the implementation of the operational snow analysis. The components in blue have been replaced by the components shown in red.

at this time and the analysis is almost identical with the first guess. At 06 UTC (upper right image), the first guess (i.e. the 12-hour forecast from 18 UTC) was updated with the increments from 00 UTC and modified through the SYNOB observations, substantially increasing SWE over Eastern Europe. The analysis at 12 UTC makes use of the first guess from 06 UTC and the satellite observations, which reduce SWE along the edges, especially over Southern Sweden (lower left image). Although it was found that the satellite data improve the SWE analysis (Drusch et al. (2004) and Drusch (2005)) the impact on the (weather) forecast quality is neutral.

Another important snow parameter for NWP applications is fractional snow coverage. Although satellite derived data sets have been available for more than a decade, snow cover is diagnosed from the (analysed) snow water equivalent. A number of parameterizations is available through the reviewed literature, Fig. 11 shows four of them. Large differences between the individual parameterizations can be seen and one can assume that they have been tuned to fit the different global circulation models at their individual spatial resolutions. The ECMWF model is unique in that fractional snow coverage is quite insensitive to SWE over a large dynamical range. In order to obtain a more realistic feedback between snow and the atmosphere it may be necessary to analyse snow coverage or modify the parameterization shown in Fig. 11 by taking the model resolution into account.

## 4 Synergies with the Atmospheric Analysis

Passive microwave observations could potentially be used over land if the background emission would be known (see Karbou et al., this issue). Figure 12 shows time series of surface emissivities at 19 GHz over the Central Facility site in Oklahoma, US, for the period from June 15 to July 18. Curve (1) was obtained by dividing observed Special Sensor Microwave / Imager (SSM/I) brightness temperatures (h-polarization) by observed surface temperatures. For (2) an atmospheric correction based on temperature and humidity profiles has been applied, for (3) a correction for the effects of an attenuating vegetation layer has been performed (Drusch et al. (2001)). (3) reflects a backward retrieval and gives an estimate of the soil emissivity, which has also been computed by a forward model based on measured soil moisture, temperature and observed soil parameters (4).

The backward retrieval (3) and the forward model (4), which are based on totally independent observations give very similar results. Although the forward model is probably not accurate enough to provide emissivities that

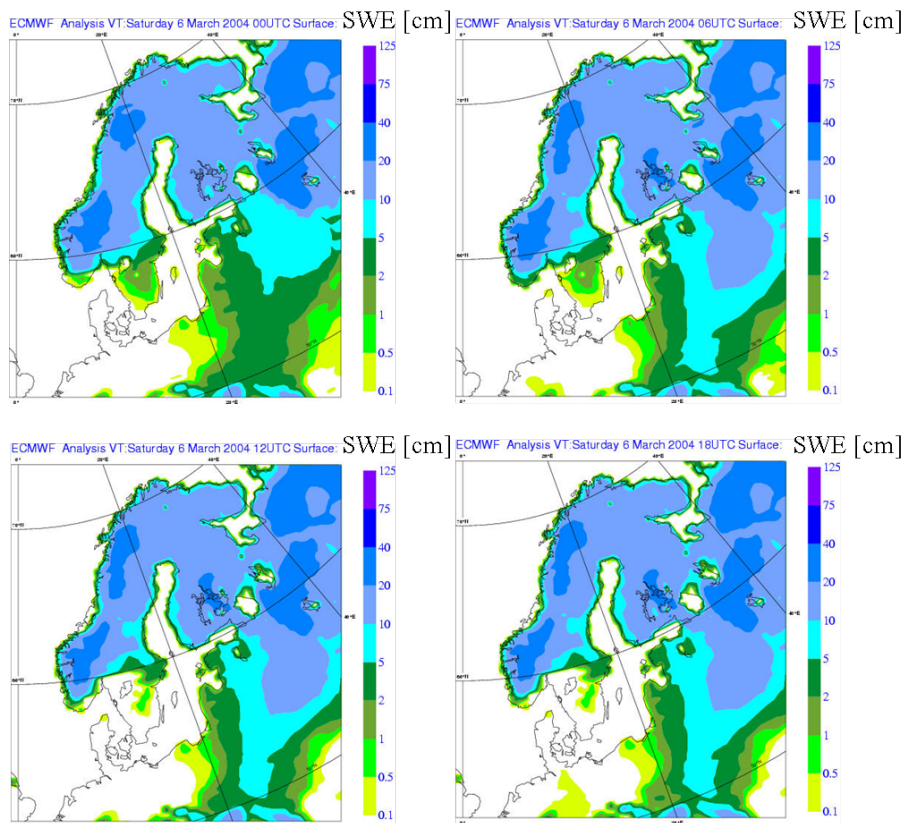


Figure 10: Example of the 6-hour snow water equivalent analyses in the 12-hour 4D-Var system.

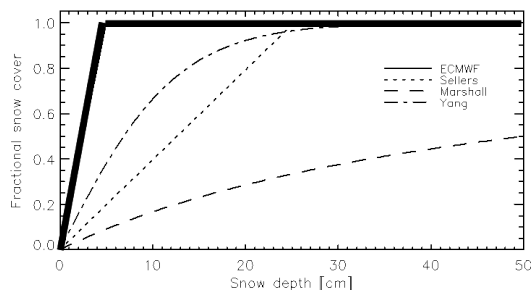


Figure 11: Fractional snow coverage as a function of SWE: Parameterizations used by ECMWF, Sellers et al. (1996), Yang et al. (1997), and Marshall et al. (1994).

can be used directly in the atmospheric 4D-Var (Drusch et al. (2001)), the emissivities can be used to constrain the atmospheric analysis, e.g. through their tendencies.

## 5 Summary

Advances in using satellite observations over land require changes to the current forecast model and to the data assimilation system. To better utilize the vast amount of satellite observations the ECMWF model should be updated with a multi-layer snow model and a subgrid snow distribution model to enable separate analyses for SWE and fractional snow cover. In addition, a dynamic vegetation model is needed to provide a first guess

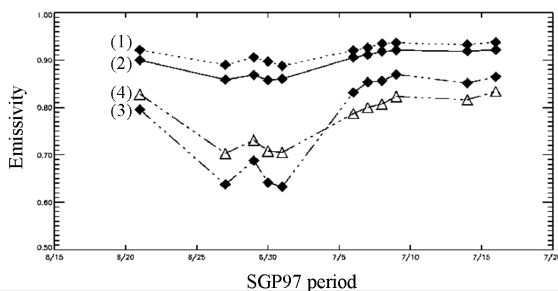


Figure 12: Surface emissivities during SGP97 for the Central Facility Site.

for the assimilation of leaf area index or similar products derived from optical and near infra red instruments (e.g. MODIS, MERIS, or AVHRR). A prototype for such an analysis system has been developed and successfully tested within the GEOLAND project (Jarlan et al. (2007)). In terms of soil water content, it would be desirable to add a routing scheme to predict (and monitor) streamflow in rivers. Data on terrestrial water storage from GRACE (Gravity Recovery and Climate Experiment) would also be helpful to further constrain the system.

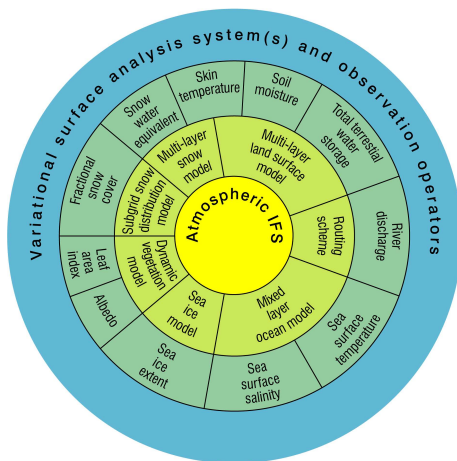


Figure 13: Schematic view on the components of an advanced surface analysis system.

The Kalman filter is a powerful tool, which can eventually be used to analyse soil moisture, SWE, and fractional snow coverage with an assimilation window of 12-hour in parallel to the atmospheric 4D-Var. In addition, the land surface system can be run 'offline' with a long cut-off time and a long window of several days. Such a system would enable the analyses of vegetation properties and terrestrial water storage. A schematic view of an advanced model system is given in Fig. 13.

It is obvious that an improved surface analysis is a value in itself as it provides more accurate initial conditions for the forecasting system. As already mentioned in the 'Introduction', land surface parameters are also of great interest to many scientists and policy makers outside the NWP community. In addition, we hope to increase the number of satellite observations used in the atmospheric 4D-Var analysis over land through a better representation of the land surface and subsequently reliable estimates of emissivities and reflectances.

## References

Daley, R. (1991). Atmospheric Data Analysis. Cambridge University Press, Cambridge, UK.

- Drusch, M., E. Wood, and T. Jackson (2001). Vegetative and atmospheric corrections for soil moisture retrieval from passive microwave remote sensing data: Results from the Southern Great Plains Hydrology Experiment 1997. *J. Hydromet.*, *2*, 181–192.
- Drusch, M., D. Vasilievic, and P. Viterbo (2004). ECMWF's global snow analysis: Assessment and revision based on satellite observations. *J. Appl. Met.*, *43*, 1282–1294.
- Drusch, M., E. Wood, and H. Gao (2005). Observation operators for the direct assimilation of TRMM Microwave Imager retrieved soil moisture. *Geophys. Res. Lett.*, *32*, L19503, doi:10.1029/2005GL023623.
- Drusch, M. (2005). Observation operators for the direct assimilation of TRMM Microwave Imager retrieved soil moisture. *Proceedings of the ECMWF/ELDAS workshop, ECMWF*, 105–114.
- Drusch, M., and P. Viterbo (2007). Soil moisture analysis in ECMWF's Integrated Forecast System - Assimilation of screen level variables. *Mon. Wea. Rev.*, *135*, 300–314.
- Drusch, M. (2007). Initializing numerical weather prediction models with satellite derived surface soil moisture: Data assimilation experiments with ECMWF's Integrated Forecast System and the TMI soil moisture data set. *J. Geophys. Res.*, *112*, D03102, doi:10.1029/2006JD007478.
- Drusch, M., T. Holmes, and G. Balsamo (2007). Comparing ERA-40 based L-band brightness temperatures with Skylab observations: A calibration / validation study using the Community Microwave Emission Model. *J. Hydromet.*, *submitted*.
- Ferranti, L., and P. Viterbo (2006). The European summer of 2003: Sensitivity to soil water initial conditions. *J. Climate*, *19*, 3659–3680.
- Hess, R. (2001). Assimilation of screen-level observations by variational soil moisture analysis. *Meteorol. Atmos. Phys.*, *39*, 1729–1735.
- Holmes, T., M. Drusch, J.-P. Wigneron, and R. deJeu (2007). A global simulation of microwave emission: Error structures based on output from ECMWF's operational Integrated Forecast System. *IEEE Trans. Geo. Rem. Sens.*, *37*, 2136–2151.
- Jarlan, L., G. Balsamo, S. Lafont, A. Beljaars, J.-C. Calvet, and E. Mognin (2007). Analysis of leaf area index in the ECMWF land surface model and impact on latent and carbon fluxes. Application to West Africa. *submitted to J. Geophys. Res.*
- Kerr, Y.H., P. Waldteufel, J.-P. Wigneron, J.-M. Martinuzzi, J. Font and M. Berger (2001). Soil moisture retrieval from space: The Soil Moisture and Ocean Salinity (SMOS) Mission. *IEEE Trans. Geo. Rem. Sens.*, *39*, 1729–1735.
- Koster, R. and The GLACE Team (2004). Regions of strong coupling between soil moisture and precipitation. *Science*, *305*, 1138–1140.
- Marshall, S., J. Rhoads, and G. Glatzmaier (1994). Snow hydrology in a general circulation model. *J. Climate*, *7*, 1251–1269.
- Schär, C., D. Luethi, U. Beyerle, and E. Heise (1999). The soil - precipitation feedback: A process study with a regional climate model. *J. Climate*, *12*, 722–741.
- Sellers, P., D. Randall, G. Collatz, J. Berry, C. Field, D. Dazlich, C. Zhang, G. Collelo, and L. Bounouna (1996). A revised land surface parameterization (SiB2) for atmospheric GCMs, Part I: model formulation. *J. Climate*, *9*, 676–705.
- Seuffert, G., H. Wilker, P. Viterbo, M. Drusch and J.F. Mahfouf (2004). On the usage of screen level parameters and microwave brightness temperature for soil moisture analysis. *J. Hydromet.*, *5*, 516–531.



- Seuffert, G., P. Gross, C. Simmer, and E.F. Wood (2002). The influence of hydrologic modelling on the predicted local weather: Two-way coupling of a mesoscale weather prediction model and a land surface hydrologic model. *J. Hydromet.*, 3, 505–523.
- Shukla, J. and Y. Mintz (1982). Influence of the land surface evapotranspiration on the Earth's climate. *Science*, 215, 1498–1501.
- Wagner, W. (1998). Soil moisture retrieval from ERS scatterometer data. *Geowiss. Mitt. Heft 49, Studienrichtung Vermess., Tech. Uni. Wien*, 102 pp.
- Yang, Z.-L., R. Dickinson, A. Robock, and K. Vinnikov (1997). Validation of the snow submodel of the biosphere-atmosphere transfer scheme with Russian snow cover and meteorological observational data. *J. Climate*, 10, 353–373.